Semnan University

Progress in Physics of Applied Materials

journal homepage: https://ppam.semnan.ac.ir/

A Graphene and Nickel-Cobalt Metal Organic Framework Composite as a high-performance electrode material for supercapacitor application

S. Salehi *, I. Karimzadeh

Department of Physics, Faculty of Science, Central Tehran Branch, Islamic Azad University, Tehran, Iran

ARTICLE INFO

Article history:
Received: 7 December 2023
Revised: 31 December 2023
Accepted: 31 December 2023

Keywords:
Electrodeposition
Ni, Co-MOF-G/ NF
Supercapacitors
Porous materials

ABSTRACT

A high-performance Ni, Co-MOF-G/nickel foam was fabricated using a novel electrodeposition method and used as an electrode material for a supercapacitor application. Structural tests including powder X-ray diffraction (XRD), Fourier transform infrared spectroscopy (FT-IR), and Raman results affirmed the formation of the electrode active materials. Scanning electron microscopy (SEM) images showed a flower-like Ni, Co-MOF inside graphene sheets forming a composition of active materials on the nickel foam substrate. The electrochemical performance of the Ni, Co-MOF-G/ Nickel foam was examined using cyclic voltammetry (CV), galvanostatic charge/discharge (GCD), and electrochemical impedance spectroscopy (EIS). The prepared electrode delivered approvable specific capacitance of 1158 F g^{-1} at the current density of 2 A g^{-1} in three molar potassium hydroxides. Excellent storage capacity of the fabricated electrode is attributed to the synergetic effects of bi-metal metal organic frameworks (Ni, Co-MOF) with porous carbon materials (graphene).

1. Introduction

Due to increasing of the global warming, the energy storage devices have become a prominent research topic in recent decades [1]. Supercapacitors are new type of energy storage device due to short charging time, long cycle life, and high thermal stability [2]. The innovative carbon materials are being investigated as electrode materials for supercapacitors lately [3]. Due to its important advantages, such as considerable surface area, great chemical stability, relatively low cost, well controlled pore structure, and the suitable electrical conductivity, they have been recently used as nanoporous carbon materials for supercapacitors [4].

Metal-Organic Frameworks (MOFs) which formed by metal centers in connection with bridged organic linkers, have been the target of tremendous efforts in the last two decades [5]. As coordinated polymers, MOFs are the most versatile porous material with high surface area due to the variation of the metal ions and organic linkers. Metal organic frameworks are recently used as electrode materials for supercapacitors but their low electrical conductivity, and limited storage density barrier its usage as supercapacitors [6]. Assembling MOFs with conductive carbon product to produce a new MOF-based composite can solve the issue [7].

For example, Beka et al. investigated on bi-metal-MOFs with graphene which has capability to enhance electrode materials for supercapacitor application [8]. Saraf et al. showed Cu-MOFs@GO as pseudocapacitors materials with a capacitance of 685.33 F g^{-1} at 1.6 A g^{-1} [9]. Kim et al. reported Ni Metal Organic Framework/Reduced Graphene Oxide Composites for supercapacitors, Ni-MOF/rGO composite was found to have a high capacitance of 1154.4 F/g at 1 A/g [10].

There have been some conventional synthesis methods for preparation of MOF electrode materials such as solvothermal, chemical, and sonochemical so far [11]. Direct electrodeposition synthesis of MOF onto electrode substrate is a new bright method for preparing supercapacitor electrode and electrode material simultaneously [12]. Fast, easy, direct, and binder-less

* Corresponding author.
E-mail address: Shiva.salehi10@gmail.com

Cite this article as:
Salehi, S., and Karimzadeh, I., 2023. A Graphene and Nickel-Cobalt Metal Organic Framework Composite as a high-performance electrode material for supercapacitor application. *Progress in Physics of Applied Materials*, *3*(2), pp. 211-216. DOI: 10.22075/PPAM.2023.32594.1075

process of electrodeposition synthesis are the other advantages of this method [13]. This one-step method used to produce Ni, Co-MOF-G/Nickel foam in this work.

2. Experimental

2.1. Chemicals

Cobalt (II) nitrate nonahydrate [Co $(NO_3)_2 6\ H_2O$], nickel (II) nitrate hexahydrate [Ni $(NO_3)_2 6\ H_2O$], terephthalic acid (H_2BDC), graphene and dimethylformamide (DMF) received from Merck company. The electrolyte solution was prepared using a mixture of H_2BDC (0.2 g), Ni $(NO_3)_2 6\ H_2O$ (0.15 g), Co $(NO_3)_2 6\ H_2O$ (0.15 g) and graphene (1 mg) in 50 cc of DMF solution. The mixture was sonicated for 5 min, and then the homogeneous solution obtained.

2.1.1. Synthesis of Ni, Co-MOF-G/Nickel foam

Indirect electrochemical procedure was applied to seeds and grow thin composite Ni, Co-MOF-G on to nickel foam substrate. In this regard, a two-electrode system was set up by applying nickel foam as a cathode and graphite rod as an anode. The electrochemical procedure was run by constant current density into the cell. After a short time of deposition, a thin film was deposited on a 1cm ∗ 1 cm nickel substrate. The optimized time, current density, and cell temperature were achieved to be 10 min, 2 mA/cm^2 and 40 °C respectively. The prepared electrode kept at vacuum oven to dry at 110 °C for 8 h. The schematic procedure illustration shown in Figure 1.

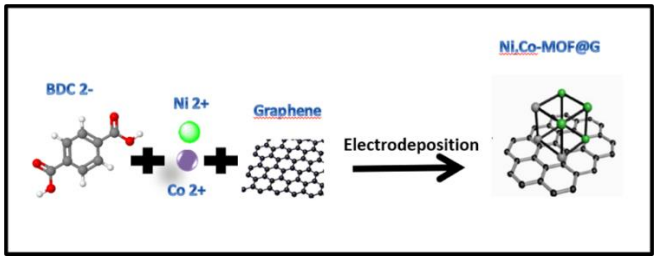

Fig. 1. schematic illustration of the synthesis procedure.

2.2. Materials characterizations

XRD patterns of the fabricated Ni, Co-MOF-G/Ni foam and pure H_2BDC powders obtained using Philips X-pert diffractometer with monochromatic CuKα radiation (λ = 1.54056Å). Fourier transform infrared (FT-IR) spectra recorded with Bruker Vector 22 FT-IR spectrometer within in the range number of 400-4000 cm^{-1}. Raman spectroscopy obtained using a DXR Smart Raman . Morphological features of the prepared electrode were depicted by scanning electron microscopy (SEM, model: Zeiss Mira 3-XMU). Cyclic voltammetry (CV), chronopotentiometry and EIS were run by autolab potentiostat/galvanostat in three molar potassium hydroxide electrolytes. In the three-electrode set-up, Ni, Co-MOF-G/nickel foam was applied as the working electrode and graphite rod as a counter electrode and Ag/AgCl (saturated KCl) as a reference electrode.

2.3. Structural and electrochemical tests

The electrochemical analysis of the fabricated electrode was run by a three-electrode set-up including; cyclic voltammetry (CV), galvanostatic charge–discharge (GCD), and electrochemical impedance spectroscopy (EIS), performed via IVIUM Vertex potentiostat/galvanostat. The nickel foam, Ag/AgCl, and graphite rod were employed as working electrode, reference electrode, and counter electrode, respectively. The conductive electrolyte was aqueous solution of three molar potassium hydroxide. Cyclic voltammograms were recorded within the range of -0.1 to 0.6 V at various scan rates. Also, GCD curves were performed at the same electrolyte solution with different current densities of 2, 5, 7, 10,15, and 20 A/g. The EIS test was examined by applying the AC voltage of 10 mV amplitude and the applied frequency was at the range of 0.01 Hz - 100 kHz. The loaded electrode active material weighted 4.2 mg.

The specific capacitances were measured by GCD curves via Eq. 1 [22]:

$$C = I \times \Delta t / m \times \Delta V \quad (1)$$

In the formula, C is the specific capacitance (F g^{-1}), m is the mass of the active materials (g), ΔV means the potential window (V), I refers to the discharge current (A), and Δt is discharge time (second).

3. Results and discussion

3.1. XRD

Fig. 2 shows the XRD pattern of fabricated Ni, Co-MOF-G composite powder. The first two sharpest diffraction peaks which are located at 2θ = 9.7° and 2θ = 16.3° are identified as the (100) and (101) planes of Ni-MOF material [14]. The diffraction peak at 2θ = 26.3° is corresponded to (002) plane of the graphene which reveals the graphene induce in the composite structure [15,16]. Moreover, presence of G does not change the MOF structure. All the evidence declares that the Ni, Co-MOF material synergism with graphene and seeds and growth simultaneously. Also, no unexpected diffraction peak observed confirming no unwanted phase formation during the reaction.

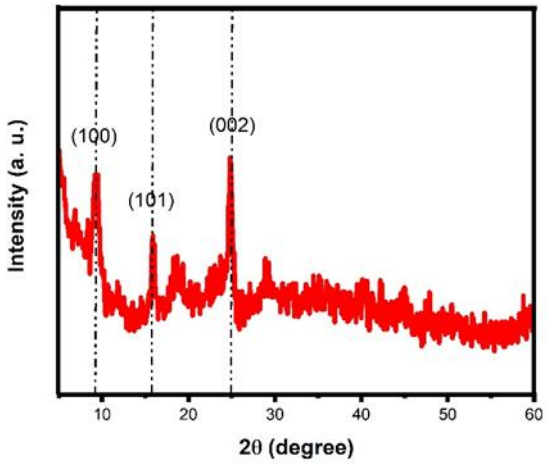

Fig. 2. XRD pattern of the fabricated Ni, Co-MOF-G.

3.2. FT-IR

To distinguish the presence of organic compounds and the formation of new functional group, Fourier transform infrared (FT-IR) spectroscopy was utilized. Figure 3 shows the FT-IR spectra of the Ni, Co-MOF-G powder and bare BDC powder. The characteristic bands of H_2BDC are υC=O at 1686 cm^{-1} and δC=O at 524 cm^{-1}, which are not detected in Ni, Co-MOF-G, confirm the absence of H_2BDC in the composite structure [17]. The absorption band located at 3400 cm^{-1} refers to O-H stretching band of water molecule [18]. Two sharp absorption bands situated at 1549.4 cm^{-1} and 1398.1 cm^{-1} imply asymmetric stretching and symmetric stretching modes of the coordinated (–COO–) group, respectively [19]. FT-IR spectra of the fabricated electrode is in good agreement with published paper [14].

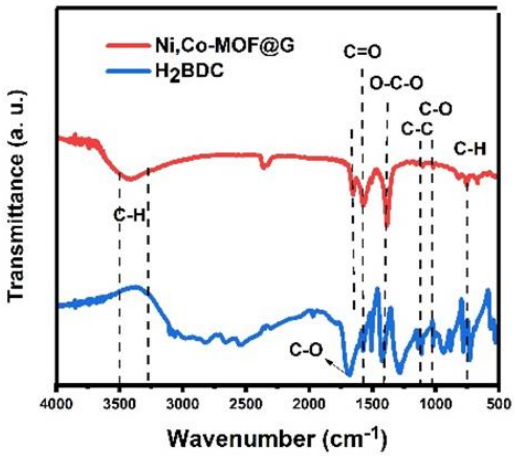

Fig. 3. FT-IR spectrum of the fabricated Ni, Co-MOF-G, and H_2BDC powders.

3.3. Raman

To further affirmation of inducing graphene in the structure, Raman spectroscopy was recorded for Ni, Co-MOF/G powder. Raman spectrum within the wavenumber range of 800 –2000 cm^{-1} is presented in Figure 4. In sample spectrum, a peak at 1347 cm^{-1} attributing to D band and a strong peak at 1580 cm^{-1} attributing to G band were observed [20]. These two characteristic bands correspond to the G (graphite) and D (defects and disorder) for carbon-based composites [21]. These results confirm the presence of graphene in the Ni, Co-MOF-G composite.

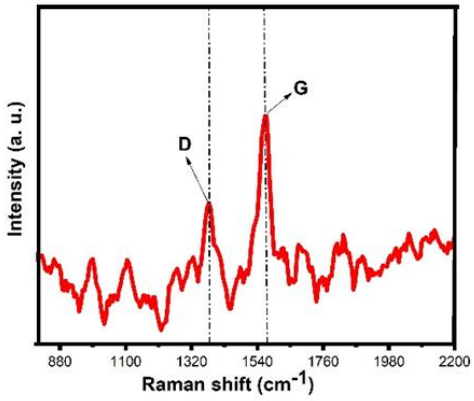

Fig. 4. Raman spectra of Ni, Co-MOF-G powder.

3.4. Surface morphology

SEM images of the Ni, Co-MOF-G are given in Figure 5. SEM images are presented at different scale magnification. Figure 5a shows the top-view of the nickel foam covered with deposited Ni, Co-MOF-G. In Figure 5b the flower-like crystalline structure of the composite can be seen. Figure 5c and d show the electrode at smaller scale in which the dense nano-sheets of Ni, Co-MOF slightly distributed among graphene sheets.

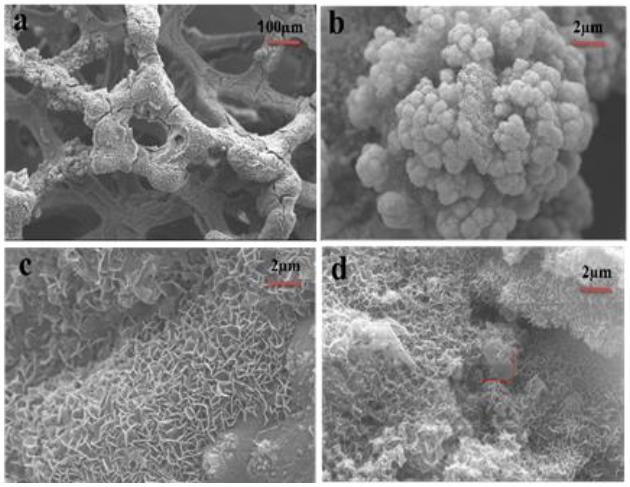

Fig. 5. (a-d) SEM images and (d) EDS data of Ni, Co-MOF-G/Ni foam.

3.5. Charge storage tests

3.5.1. Cyclic voltammetry (CV)

The electrochemical evaluation of Ni, Co-MOF-G/Ni foam electrode was done by cyclic voltammetry (CV) technique at various scan rates of 5 to 100 mV s^{-1}, with potential windows of 0-0.6V in 3 M KOH solution, as shown in Figure 6. It can be observed that in Ni, Co-MOF-G/Ni profile two oxidation peaks appear in each scan rate. These curves display semi-angular shapes due to EDLC and the pseudocapacitance affection simultaneously [19,20]. These phenomena caused by synergistic effects between pseudocapacitive Ni, Co-MOF and electric double layer capacitive graphene product of composite [24].

3.5.2. Galvanostatic charge-discharge (GCD)

To evaluate the capacitive performance of the prepared electrode, Galvanostatic charge-discharge (GCD) test was also run in the potential window of 0 - +0.45 V at different applied current densities from 2 A g^{-1} to 20 A g^{-1} in 3 M KOH solution (Figure 7). As it can be seen, by initiating charging process of the Ni, Co-MOF-G/Ni foam at all current densities, the potential increases rapidly, showing the capacitive charge storage mechanism [25]. In discharge process by applying the current densities at lower rate of current density, the discharge time increases implying better charge capacity of the electrode at 2 A/g [26]. Specific capacitance of the Ni/Co-MOF-G/Ni foam measured 1158 F/g at 2 A/g using equation 1.

3.5.3. EIS

Electrochemical impedance spectroscopy (EIS) measurements applied to indicate the electrical resistance of the fabricated electrode. Figure 8 depicts the Nyquist plots of the Ni, Co-MOF-G/Ni foam electrodes measured in the frequency range from 0.01 Hz to 100 kHz. At the high-frequency region, the intersection point of the semi-circle with the real impedance (Z0 axis) is contributed to the equivalent series resistance (ESR) [24]. ESR is the combination of various resistance including ionic resistance of the electrolyte, intrinsic resistance of the electrode active composite materials, and electrolyte/electrode contact resistance [28]. The measured ESR of the Ni, Co-MOF-G/Ni foam is 0.79 Ω.

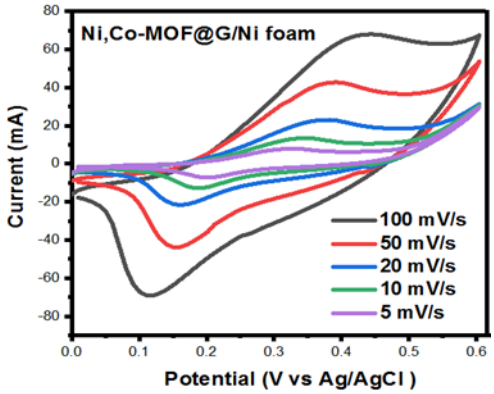

Fig. 6. Cyclic voltammetry curves of the Ni, Co-MOF-G/Ni foams, at the scan rates of 5, 10, 20, 50, and 100 m V s^{-1}.

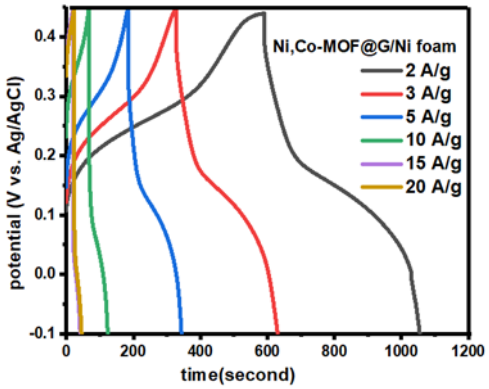

Fig. 7. GCD curves of Ni, Co-MOF-G/Ni foams at current densities of 2, 3, 5, 10, 15, and 20 A g^{-1}.

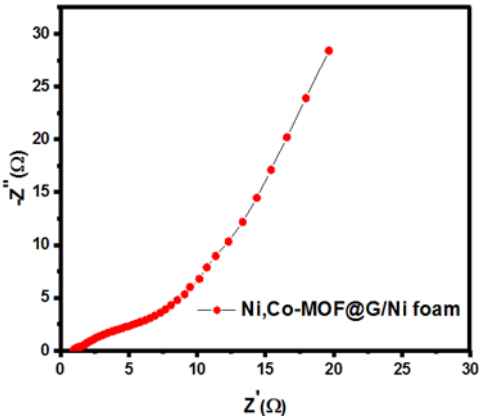

Fig. 8. Nyquist plots of Ni, Co-MOF-G/Ni foam electrodes at the frequency range of 0.01 Hz to 100 kHz.

4. Conclusions

In summary, binder-free Ni, Co-MOF-G/Ni foam was successfully fabricated by a novel and fast reductive electrodeposition method. Fabricated electrode showed a flower-like morphology with dense nanosheet aggregated in graphene sheets. Structural tests including FT-IR, Raman and XRD properly proved the formation of MOF/composite electrode active materials and the existence of graphene inside the structure. Electrochemical analyses including CV, GCD, and EIS showed the great supercapacitive behavior of the fabricated electrode implying the electrode can be well used in supercapacitor devices. The measured specific capacitance of the Ni/Co-MOF@G/Ni foam nanocomposite electrode is 1158 F/g at 2 A/g.

Acknowledgements

There is nothing to acknowledgement.

Conflicts of Interest

The author declares that there is no conflict of interest regarding the publication of this article.

References

[1] Zhu, J., Chen, X., Thang, A.Q., Li, F.L., Chen, D., Geng, H., Rui, X. and Yan, Q., 2022. Vanadium-based metal-organic frameworks and their derivatives for electrochemical energy conversion and storage. *SmartMat*, *3*(3), pp.384-416.

[2] Gu, Y., Du, W., Liu, X., Gao, R., Liu, Y., Ma, H., Xu, J. and Wei, S., 2020. Matching design of high-performance electrode materials with different energy-storage mechanism suitable for flexible hybrid supercapacitors. *Journal of Alloys and Compounds*, *844*, p.156196.

[3] Krishnan, P. and Biju, V., 2021. Reduced graphite oxide-pure water supercapacitor: A futuristic water based energy storage device. *Physica E: Low-dimensional Systems and Nanostructures*, *126*, p.114452.

[4] Zhao, J. and Burke, A.F., 2021. Electrochemical capacitors: performance metrics and evaluation by testing and analysis. *Advanced Energy Materials*, *11*(1), p.2002192.

[5] Chen, H.Y., Huo, Y.Q., Cai, K.Z. and Teng, Y., 2021. Controllable preparation and capacitance performance of bimetal Co/Ni-MOF. *Synthetic Metals*, *276*, p.116761.

[6] Srinivasan, R., Elaiyappillai, E., Nixon, E.J., Lydia, I.S. and Johnson, P.M., 2020. Enhanced electrochemical behaviour of Co-MOF/PANI composite electrode for supercapacitors. *Inorganica chimica acta*, *502*, p.119393.

[7] Anithabanu, P. and Vaidyanathan, V.G., 2021. The water soluble zinc based metal-organic frameworks (Zn-MOFs) as potential inhibitors for collagen fibrillogenesis. *International Journal of Biological Macromolecules*, *190*, pp.56-60.

[8] Beka, L.G., Bu, X., Li, X., Wang, X., Han, C. and Liu, W., 2019. A 2D metal–organic framework/reduced graphene oxide heterostructure for supercapacitor application. *RSC advances*, *9*(62), pp.36123-36135.

[9] Saraf, M., Rajak, R. and Mobin, S.M., 2016. A fascinating multitasking Cu-MOF/rGO hybrid for high performance supercapacitors and highly sensitive and selective electrochemical nitrite sensors. *Journal of Materials Chemistry A*, *4*(42), pp.16432-16445.

[10] Kim, J., Park, S.J., Chung, S. and Kim, S., 2020. Preparation and capacitance of Ni metal organic framework/reduced graphene oxide composites for supercapacitors as nanoarchitectonics. *Journal of Nanoscience and Nanotechnology*, *20*(5), pp.2750-2754.

[11] Yi, B., Zhao, H., Cao, L., Si, X., Jiang, Y., Cheng, P., Zuo, Y., Zhang, Y., Su, L., Wang, Y. and Tsung, C.K., 2022. A direct mechanochemical conversion of Pt-doped metal-organic framework-74 from doped metal oxides for CO oxidation. *Materials Today Nano*, *17*, p.100158.

[12] Salehi, S., Aghazadeh, M. and Karimzadeh, I., 2022. Zn-MOF electrode material for supercapacitor applications. *Progress in Physics of Applied Materials*, *2*(1), pp.77-82.

[13] Campagnol, N., Van Assche, T., Boudewijns, T., Denayer, J., Binnemans, K., De Vos, D. and Fransaer, J., 2013. High pressure, high temperature electrochemical synthesis of metal–organic frameworks: films of MIL-100 (Fe) and HKUST-1 in different morphologies. *Journal of Materials Chemistry A*, *1*(19), pp.5827-5830.

[14] Salehi, S., Ehsani, M.H. and Aghazadeh, M., 2023. Direct electrosynthesis of Ni-, Co-, and Ni, Co-MOF onto porous support for high-performance supercapacitors. *Journal of Alloys and Compounds*, *940*, p.168885.

[15] Zhao, G., Sedki, M., Ma, S., Villarreal, C., Mulchandani, A. and Jassby, D., 2020. Bismuth subcarbonate decorated reduced graphene oxide nanocomposite for the sensitive stripping voltammetry analysis of Pb (II) and Cd (II) in water. *Sensors*, *20*(21), p.6085.

[16] Vijayan, S., Narasimman, R. and Prabhakaran, K., 2016. A carbothermal reduction method for the preparation of nickel foam from nickel oxide and sucrose. *Materials Letters*, *181*, pp.268-271.

[17] Salehi, S., Ehsani, M.H. and Aghazadeh, M., 2022. Novel electrodeposition of bud-like cobalt/zinc metal-organic-framework onto nickel foam as a high-performance binder-free electrode material for supercapacitor applications. *Materials Letters*, *319*, p.132282.

[18] Jiao, Y., Pei, J., Yan, C., Chen, D., Hu, Y. and Chen, G., 2016. Layered nickel metal–organic framework for high performance alkaline battery-supercapacitor hybrid devices. *Journal of Materials Chemistry A*, *4*(34), pp.13344-13351.

[19] Serhan, M., Jackemeyer, D., Long, M., Sprowls, M., Perez, I.D., Maret, W., Chen, F., Tao, N. and Forzani, E., 2020. Total iron measurement in human serum with a novel smartphone-based assay. *IEEE Journal of Translational Engineering in Health and Medicine*, *8*, pp.1-9.

[20] Cheng, J., Liang, J., Dong, L., Chai, J., Zhao, N., Ullah, S., Wang, H., Zhang, D., Imtiaz, S., Shan, G. and Zheng, G., 2018. Self-assembly of 2D-metal–organic framework/graphene oxide membranes as highly efficient adsorbents for the removal of Cs^+ from aqueous solutions. *RSC advances*, *8*(71), pp.40813-40822.

[21] More, M.S., Bodkhe, G.A., Ingle, N.N., Singh, F., Tsai, M.L., Kim, M. and Shirsat, M.D., 2023. Metal-organic framework (MOF)/reduced graphene oxide (rGO) composite for high performance CO sensor. *Solid-State Electronics*, *204*, p.108638.

[22] Salehi, S., Ehsani, M.H., Aghazadeh, M., Badiei, A. and Ganjali, M.R., 2022. Electrodeposition of binderless Ni, Zn-MOF on porous nickel substrate for high-efficiency supercapacitors. *Journal of Solid State Chemistry*, *316*, p.123549.

[23] Cherusseri, J., Pandey, D. and Thomas, J., 2020. Symmetric, asymmetric, and battery-type supercapacitors using two-dimensional nanomaterials and composites. *Batteries & Supercaps*, *3*(9), pp.860-875.

[24] Iqbal, M.Z., Faisal, M.M. and Ali, S.R., 2021. Integration of supercapacitors and batteries towards high-performance hybrid energy storage devices. *International Journal of Energy Research*, *45*(2), pp.1449-1479.

[25] Wan, J., Li, J., Xiao, Z., Tang, D., Wang, B., Xiao, Y. and Xu, W., 2020. Transition bimetal based mof nanosheets for robust aqueous Zn battery. *Frontiers in Materials*, *7*, p.194.

[26] Majumdar, D., 2021. Review on current progress of MnO2-based ternary nanocomposites for supercapacitor applications. *ChemElectroChem*, *8*(2), pp.291-336.

[27] Aghazadeh, M., Karimzadeh, I., Ahmadi, A. and Ganjali, M.R., 2018. Electrochemical grown cobalt hydroxide three-dimensional nanostructures on Ni foam as high performance supercapacitor electrode material. *Journal of Materials Science: Materials in Electronics*, *29*, pp.14567-14573.

[28] Aghazadeh, M., Karimzadeh, I. and Ganjali, M.R., 2019. Preparation and Characterization of Amine-and Carboxylic Acid-functionalized Superparamagnetic Iron Oxide Nanoparticles Through a One-step Facile Electrosynthesis Method. *Current Nanoscience*, *15*(2), pp.169-177.